whereas it inhibits POMC and CART expression in the ARC (34, 57). Reduced ghrelin secretion may decrease *NPY* mRNA levels and increase *POMC* and *CART* mRNA levels in the ARC. These findings indicated that distinct underlying mechanisms may induce cachexia-associated anorexia development in different cachexia models.

In addition to body weight loss and anorexia, patients with cancer cachexia also exhibit a reduction in physical activity corresponding to daytime activities (22, 61). Similarly, locomotor activity in the "active period" or dark phase was substantially lower in 85As2-induced cachectic rats than in control rats, whereas locomotor activity was not different between these groups during the daytime period. Reduced activity during the dark phase, but not the light phase, in cachectic rats has also been observed in other cachexia models (41, 59). Because $\dot{V}O_2$ is thought to be affected by the amount of locomotor activity, we evaluated this parameter during the daytime period. $\dot{V}O_2$, RQ, and metabolic calorie levels were significantly higher in cachectic rats than in control rats during this time period. These findings suggested that enhanced energy expenditure, in addition to anorexia, may exacerbate body weight loss caused by the decrease in adipose and muscle tissues in cachectic rats. In fact, exacerbated resting energy expenditure in patients with cancer cachexia has frequently been observed (7, 8, 21) and is in contrast to the resting energy conservation associated with starvation-induced body weight loss.

Body weight maintenance is the most important end point of any treatment for cachexia-associated anorexia. Rikkunshito therapy has been shown to be an effective anorexia treatment in several animal models (50, 57); therefore, we evaluated the effect of rikkunshito on 85As2-induced cachexia symptoms. Rikkunshito substantially ameliorated cancer cachexia symptoms, including anorexia, weight loss, decreased water intake, and reductions in FFM, TBW, and musculature in the 85As2-induced cancer cachexia rat model; however, rikkunshito did not reduce tumor growth or plasma LIF levels. These findings indicated that the anticachectic effects of rikkunshito are not related to tumor regression or LIF levels. Rikkunshito has been shown to increase the secretion of ghrelin, an orexigenic hormone (57), and also to increase ghrelin receptor (GHSR) signaling efficacy (24). GHSR is expressed in the ARC and PVN of the hypothalamus, and ligand binding stimulates NPY/AgRP neurons, thereby transducing orexigenic signals to increase food intake. Thus, rikkunshito may ameliorate anorexia by activating GHSR-NPY/AgRP orexigenic signaling in the ARC and PVN. In fact, our previous study demonstrated that rikkunshito ameliorated cisplatin-induced anorexia in rats and reversed the cisplatin-induced decrease in hypothalamic orexigenic peptide mRNA levels (*NPY* in ARC) and increase in anorexigenic peptide mRNA levels (*POMC* and *CART* in the ARC) (65). Because anorexia induced by cancer cachexia and cisplatin may involve different mechanisms, further study is required to clarify the mechanisms by which rikkunshito ameliorates cancer cachexia-induced anorexia.

In conclusion, we established novel stomach cancer cachexia rat models by implanting nude rats with MKN45cl85 and 85As2 cells, both of which were derived from the human stomach cancer cell line MKN-45. The 85As2-induced cancer cachexia model, which was generated using peritoneal dissemination-derived 85As2 cells, induced earlier and more severe cachexia than the MKN45cl85 model, which may have been caused by differences in LIF production. The 85As2 model allowed for the early evaluation of cancer cachexia parameters associated with poor patient QOL and metabolic disturbances, such as anorexia and body weight loss (including low FFM). Our findings also indicate that rikkunshito may improve QOL in patients with stomach cancer cachexia. The 85As2 model should provide a useful tool for further study of cancer cachexia pathogenesis and treatment.

ACKNOWLEDGMENTS

We thank our colleagues in our laboratory for their technical assistance and helpful comments.

GRANTS

This work was supported in part by a Grant-in-Aid for the Third-Term Comprehensive 10-Year Strategy for Cancer Control from the Ministry of Health, Labour, and Welfare, Japan; a Grant-in-Aid for Scientific Research (C) from Ministry of Education, Culture, Sports, Science, and Technology, Japan; the National Cancer Center Research and Development Fund (23-A-2, 23-A-29, 23-A-38); the Foundation for Promotion of Cancer Research in Japan; and a grant from Tsumura and Co. (Tokyo, Japan).

DISCLOSURES

Y. Uezono received grant support from Tsumura & Co. K. Terawaki and Y. Kase are employed by Tsumura & Co. Y. Sawada, Y. Kase, H. Hashimoto, M. Yoshimura, M. Suzuki, K. Miyano, Y. Sudo, S. Shiraishi, Y. Higami, K. Yanagihara, and Y. Ueta have no conflicts of interest to disclose.

AUTHOR CONTRIBUTIONS

K.T., Y. Sawada, Y. Kashiwase, H.H., M.Y., M.S., K.M., Y. Sudo, Y. Ueta, and Y. Uezono contributed to the conception and design of the research; K.T., Y. Sawada, Y. Kashiwase, H.H., M.Y., M.S., K.M., and Y. Sudo performed the experiments; K.T., Y. Sawada, Y. Kashiwase, H.H., M.Y., M.S., K.M., and Y. Sudo analyzed the data; K.T., Y. Sawada, Y. Kashiwase, H.H., M.Y., M.S., K.M., Y. Sudo, K.Y., and Y. Uezono interpreted the results of the experiments; K.T., Y. Sawada, Y. Kashiwase, H.H., and M.Y. prepared the figures; K.T. drafted the manuscript; K.T., S.S., Y.H., K.Y., Y. Ueta, and Y. Uezono edited and revised the manuscript; K.T., S.S., Y.H., K.Y., Y. Kase, Y. Ueta, and Y. Uezono approved the final version of manuscript.

REFERENCES

1. **Argilés JM, Olivan M, Busquets S, López-Soriano FJ.** Optimal management of cancer anorexia-cachexia syndrome. *Cancer Manag Res* 2: 27–38, 2010.
2. **Asp ML, Tian M, Wendel AA, Belury MA.** Evidence for the contribution of insulin resistance to the development of cachexia in tumor-bearing mice. *Int J Cancer* 126: 756–763, 2010.
3. **Auernhammer CJ, Melmed S.** Leukemia-inhibitory factor-neuroimmune modulator of endocrine function. *Endocr Rev* 21: 313–345, 2000.
4. **Bennani-Baiti N, Walsh D.** Animal models of the cancer anorexia-cachexia syndrome. *Support Care Cancer* 19: 1451–1463, 2011.
5. **Bo S, Dianliang Z, Hongmei Z, Xinxiang W, Yanbing Z, Xiaobo L.** Association of interleukin-8 gene polymorphism with cachexia from patients with gastric cancer. *J Interferon Cytokine Res* 30: 9–14, 2010.
6. **Bodine SC, Latres E, Baumhueter S, Lai VK, Nunez L, Clarke BA, Poueymirou WT, Panaro FJ, Na E, Dharmarajan K, Pan ZQ, Valenzuela DM, DeChiara TM, Stitt TN, Yancopoulos GD, Glass DJ.** Identification of ubiquitin ligases required for skeletal muscle atrophy. *Science* 294: 1704–1708, 2001.
7. **Bosaeus I, Daneryd P, Svanberg E, Lundholm K.** Dietary intake and resting energy expenditure in relation to weight loss in unselected cancer patients. *Int J Cancer* 93: 380–383, 2001.
8. **Cao DX, Wu GH, Zhang B, Quan YJ, Wei J, Jin H, Jiang Y, Yang ZA.** Resting energy expenditure and body composition in patients with newly detected cancer. *Clin Nutr* 29: 72–77, 2010.
9. **Chance WT, Balasubramaniam A, Borchers M, Fischer JE.** Refractory hypothalamic adenylate cyclase in anorectic tumor-bearing rats: implications for NPY-induced feeding. *Brain Res* 691: 180–184, 1995.

10. **Chance WT, Balasubramaniam A, Dayal R, Brown J, Fischer JE.** Hypothalamic concentration and release of neuropeptide Y into microdialysates is reduced in anorectic tumor-bearing rats. *Life Sci* 54: 1869–1874, 1994.
11. **Chance WT, Balasubramaniam A, Thompson H, Mohapatra B, Ramo J, Fischer JE.** Assessment of feeding response of tumor-bearing rats to hypothalamic injection and infusion of neuropeptide Y. *Peptides* 17: 797–801, 1996.
12. **Chance WT, Sheriff S, Kasckow JW, Regmi A, Balasubramaniam A.** NPY messenger RNA is increased in medial hypothalamus of anorectic tumor-bearing rats. *Regul Pept* 75–76: 347–353, 1998.
13. **Chang JW, Yeh KY, Shen YC, Hsieh JJ, Chuang CK, Liao SK, Tsai LH, Wang CH.** Production of multiple cytokines and induction of cachexia in athymic nude mice by a new anaplastic thyroid carcinoma cell line. *J Endocrinol* 179: 387–394, 2003.
14. **Chen SZ, Qiu ZG.** Combined treatment with GH, insulin, and indomethacin alleviates cancer cachexia in a mouse model. *J Endocrinol* 208: 131–136, 2011.
15. **Collins TJ.** ImageJ for microscopy. *BioTechniques* 43, *1* Suppl*: 25–30, 2007.*
16. **Costelli P, Muscaritoli M, Bossola M, Penna F, Reffo P, Bonetto A, Busquets S, Bonelli G, Lopez-Soriano FJ, Doglietto GB, Argilés JM, Baccino FM, Rossi Fanelli F.** IGF-1 is downregulated in experimental cancer cachexia. *Am J Physiol Regul Integr Comp Physiol* 291: R674–R683, 2006.
17. **Donohue E, Thomas A, Maurer N, Manisali I, Zeisser-Labouebe M, Zisman N, Anderson HJ, Ng SS, Webb M, Bally M, Roberge M.** The autophagy inhibitor verteporfin moderately enhances the antitumor activity of gemcitabine in a pancreatic ductal adenocarcinoma model. *J Cancer* 4: 585–596, 2013.
18. **dupont NC, Wang K, Wadhwa PD, Culhane JF, Nelson EL.** Validation and comparison of luminex multiplex cytokine analysis kits with ELISA: determinations of a panel of nine cytokines in clinical sample culture supernatants. *J Reprod Immunol* 66: 175–191, 2005.
19. **Ebrahimi B, Tucker SL, Li D, Abbruzzese JL, Kurzrock R.** Cytokines in pancreatic carcinoma: correlation with phenotypic characteristics and prognosis. *Cancer* 101: 2727–2736, 2004.
20. **Evans WJ, Morley JE, Argilés J, Bales C, Baracos V, Guttridge D, Jatoi A, Kalantar-Zadeh K, Lochs H, Mantovani G, Marks D, Mitch WE, Muscaritoli M, Najand A, Ponikowski P, Rossi Fanelli F, Schambelan M, Schols A, Schuster M, Thomas D, Wolfe R, Anker SD.** Cachexia: a new definition. *Clin Nutr* 27: 793–799, 2008.
21. **Falconer JS, Fearon KC, Plester CE, Ross JA, Carter DC.** Cytokines, the acute-phase response, and resting energy expenditure in cachectic patients with pancreatic cancer. *Ann Surg* 219: 325–331, 1994.
22. **Fouladiun M, Körner U, Gunnebo L, Sixt-Ammilon P, Bosaeus I, Lundholm K.** Daily physical-rest activities in relation to nutritional state, metabolism, and quality of life in cancer patients with progressive cachexia. *Clin Cancer Res* 13: 6379–6385, 2007.
23. **Fujitsuka N, Asakawa A, Hayashi M, Sameshima M, Amitani H, Kojima S, Fujimiya M, Inui A.** Selective serotonin reuptake inhibitors modify physiological gastrointestinal motor activities via 5-HT2c receptor and acyl ghrelin. *Biol Psychiatry* 65: 748–759, 2009.
24. **Fujitsuka N, Asakawa A, Uezono Y, Minami K, Yamaguchi T, Niijima A, Yada T, Maejima Y, Sedbazar U, Sakai T, Hattori T, Kase Y, Inui A.** Potentiation of ghrelin signaling attenuates cancer anorexia-cachexia and prolongs survival. *Transl Psychiatry* 1: e23, 2011.
25. **Gomes MD, Lecker SH, Jagoe RT, Navon A, Goldberg AL.** Atrogin-1, a muscle-specific F-box protein highly expressed during muscle atrophy. *Proc Natl Acad Sci USA* 98: 14440–14445, 2001.
26. **Graziano F, Ruzzo A, Santini D, Humar B, Tonini G, Catalano V, Berardi R, Pizzagalli F, Arduini F, Bearzi I, Scartozzi M, Cascinu S, Testa E, Ficarelli R, Magnani M.** Prognostic role of interleukin-1beta gene and interleukin-1 receptor antagonist gene polymorphisms in patients with advanced gastric cancer. *J Clin Oncol* 23: 2339–2345, 2005.
27. **Grossberg AJ, Scarlett JM, Zhu X, Bowe DD, Batra AK, Braun TP, Marks DL.** Arcuate nucleus proopiomelanocortin neurons mediate the acute anorectic actions of leukemia inhibitory factor via gp130. *Endocrinology* 151: 606–616, 2010.
28. **Hanada R, Teranishi H, Pearson JT, Kurokawa M, Hosoda H, Fukushima N, Fukue Y, Serino R, Fujihara H, Ueta Y, Ikawa M, Okabe M, Murakami N, Shirai M, Yoshimatsu H, Kangawa K, Kojima M.** Neuromedin U has a novel anorexigenic effect independent of the leptin signaling pathway. *Nat Med* 10: 1067–1073, 2004.
29. **Harasawa S, Miyoshi A, Miwa T, et al.** Double-blind multicenter post-marketing clinical trial of TJ-43 TSUMURA Rikkunshi-to for the treatment of dysmotility-like dyspepsia. *J Clin Exp Med* 187: 207–229, 1998.
30. **Harbuz MS, Chalmers J, De Souza L, Lightman SL.** Stress-induced activation of CRF and c-fos mRNAs in the paraventricular nucleus are not affected by serotonin depletion. *Brain Res* 609: 167–173, 1993.
31. **Hashimoto H, Azuma Y, Kawasaki M, Fujihara H, Onuma E, Yamada-Okabe H, Takuwa Y, Ogata E, Ueta Y.** Parathyroid hormone-related protein induces cachectic syndromes without directly modulating the expression of hypothalamic feeding-regulating peptides. *Clin Cancer Res* 13: 292–298, 2007.
32. **Hayakawa T, Arakawa T, Kase Y, Akiyama S, Ishige A, Takeda S, Sasaki H, Uno H, Fukuda T, Higuchi K, Kobayashi K.** Liu-Jun-Zi-Tang, a kampo medicine, promotes adaptive relaxation in isolated guinea pig stomachs. *Drugs Exp Clin Res* 25: 211–218, 1999.
33. **Inokuma K, Okamatsu-Ogura Y, Omachi A, Matsushita Y, Kimura K, Yamashita H, Saito M.** Indispensable role of mitochondrial UCP1 for antiobesity effect of β_3-adrenergic stimulation. *Am J Physiol Endocrinol Metab* 290: E1014–E1021, 2006.
34. **Kojima M, Kangawa K.** Ghrelin: structure and function. *Physiol Rev* 85: 495–522, 2005.
35. **Laviano A, Meguid MM, Inui A, Muscaritoli M, Rossi-Fanelli F.** Therapy insight: Cancer anorexia-cachexia syndrome—when all you can eat is yourself. *Nat Clin Pract Oncol* 2: 158–165, 2005.
36. **Liu CM, Yang Z, Liu CW, Wang R, Tien P, Dale R, Sun LQ.** Effect of RNA oligonucleotide targeting Foxo-1 on muscle growth in normal and cancer cachexia mice. *Cancer Gene Ther* 14: 945–952, 2007.
37. **Livak KJ, Schmittgen TD.** Analysis of relative gene expression data using real-time quantitative PCR and the 2(−Delta Delta C(T)) Method. *Methods* 25: 402–408, 2001.
38. **McCarthy HD, McKibbin PE, Perkins AV, Linton EA, Williams G.** Alterations in hypothalamic NPY and CRF in anorexic tumor-bearing rats. *Am J Physiol Endocrinol Metab* 264: E638–E643, 1993.
39. **Mori M, Yamaguchi K, Abe K.** Purification of a lipoprotein lipase-inhibiting protein produced by a melanoma cell line associated with cancer cachexia. *Biochem Biophys Res Commun* 160: 1085–1092, 1989.
40. **Mori M, Yamaguchi K, Honda S, Nagasaki K, Ueda M, Abe O, Abe K.** Cancer cachexia syndrome developed in nude mice bearing melanoma cells producing leukemia-inhibitory factor. *Cancer Res* 51: 6656–6659, 1991.
41. **Murphy KT, Chee A, Trieu J, Naim T, Lynch GS.** Importance of functional and metabolic impairments in the characterization of the C-26 murine model of cancer cachexia. *Dis Model Mech* 5: 533–545, 2012.
42. **Muscaritoli M, Bossola M, Aversa Z, Bellantone R, Rossi Fanelli F.** Prevention and treatment of cancer cachexia: new insights into an old problem. *Eur J Cancer* 42: 31–41, 2006.
43. **Nomura M, Ueta Y, Serino R, Kabashima N, Shibuya I, Yamashita H.** PACAP type I receptor gene expression in the paraventricular and supraoptic nuclei of rats. *Neuroreport* 8: 67–70, 1996.
44. **Ohno T, Yanai M, Ando H, Toyomasu Y, Ogawa A, Morita H, Ogata K, Mochiki E, Asao T, Kuwano H.** Rikkunshito, a traditional Japanese medicine, suppresses cisplatin-induced anorexia in humans. *Clin Exp Gastroenterol* 4: 291–296, 2011.
45. **Oike Y, Akao M, Yasunaga K, Yamauchi T, Morisada T, Ito Y, Urano T, Kimura Y, Kubota Y, Maekawa H, Miyamoto T, Miyata K, Matsumoto S, Sakai J, Nakagata N, Takeya M, Koseki H, Ogawa Y, Kadowaki T, Suda T.** Angiopoietin-related growth factor antagonizes obesity and insulin resistance. *Nat Med* 11: 400–408, 2005.
46. **Okada S, Okusaka T, Ishii H, Kyogoku A, Yoshimori M, Kajimura N, Yamaguchi K, Kakizoe T.** Elevated serum interleukin-6 levels in patients with pancreatic cancer. *Jpn J Clin Oncol* 28: 12–15, 1998.
47. **Pan W, Kastin AJ, Brennan JM.** Saturable entry of leukemia inhibitory factor from blood to the central nervous system. *J Neuroimmunol* 106: 172–180, 2000.
48. **Paxinos G, Watson C.** *The Rat Brain in Stereotaxic Coordinatesed.* Sydney, Australia: Academic, 1982.
49. **Reed SA, Sandesara PB, Senf SM, Judge AR.** Inhibition of FoxO transcriptional activity prevents muscle fiber atrophy during cachexia and induces hypertrophy. *FASEB J* 26: 987–1000, 2012.
50. **Scarlett JM, Zhu X, Enriori PJ, Bowe DD, Batra AK, Levasseur PR, Grant WF, Meguid MM, Cowley MA, Marks DL.** Regulation of agouti-related protein messenger ribonucleic acid transcription and peptide

secretion by acute and chronic inflammation. *Endocrinology* 149: 4837–4845, 2008.

51. **Scott HR, McMillan DC, Crilly A, McArdle CS, Milroy R.** The relationship between weight loss and interleukin 6 in non-small-cell lung cancer. *Br J Cancer* 73: 1560–1562, 1996.
52. **Smith DL Jr, Johnson MS, Nagy TR.** Precision and accuracy of bioimpedance spectroscopy for determination of in vivo body composition in rats. *Int J Body Compos Res* 7: 21–26, 2009.
53. **Soda K, Kawakami M, Kashii A, Miyata M.** Manifestations of cancer cachexia induced by colon 26 adenocarcinoma are not fully ascribable to interleukin-6. *Int J Cancer* 62: 332–336, 1995.
54. **Sun F, Sun Y, Yu Z, Zhang D, Zhang J, Song B, Zheng H.** Interleukin-10 gene polymorphisms influence susceptibility to cachexia in patients with low-third gastric cancer in a Chinese population. *Mol Diagn Ther* 14: 95–100, 2010.
55. **Suzuki H, Hashimoto H, Kawasaki M, Watanabe M, Otsubo H, Ishikura T, Fujihara H, Ohnishi H, Onuma E, Yamada-Okabe H, Takuwa Y, Ogata E, Nakamura T, Ueta Y.** Similar changes of hypothalamic feeding-regulating peptides mRNAs and plasma leptin levels in PTHrP-, LIF-secreting tumors-induced cachectic rats and adjuvant arthritic rats. *Int J Cancer* 128: 2215–2223, 2011.
56. **Suzuki M, Narita M, Ashikawa M, Furuta S, Matoba M, Sasaki H, Yanagihara K, Terawaki K, Suzuki T, Uezono Y.** Changes in the melanocortin receptors in the hypothalamus of a rat model of cancer cachexia. *Synapse* 66: 747–751, 2012.
57. **Takeda H, Sadakane C, Hattori T, Katsurada T, Ohkawara T, Nagai K, Asaka M.** Rikkunshito, an herbal medicine, suppresses cisplatin-induced anorexia in rats via 5-HT2 receptor antagonism. *Gastroenterology* 134: 2004–2013, 2008.
58. **Tisdale MJ.** Mechanisms of cancer cachexia. *Physiol Rev* 89: 381–410, 2009.
59. **Toledo M, Busquets S, Sirisi S, Serpe R, Orpí M, Coutinho J, Martínez R, López-Soriano FJ, Argilés JM.** Cancer cachexia: physical activity and muscle force in tumour-bearing rats. *Oncol Rep* 25: 189–193, 2011.
60. **Tominaga K, Kido T, Ochi M, Sadakane C, Mase A, Okazaki H, Yamagami H, Tanigawa T, Watanabe K, Watanabe T, Fujiwara Y, Oshitani N, Arakawa T.** The Traditional Japanese Medicine Rikkunshito Promotes Gastric Emptying via the Antagonistic Action of the 5-HT(3) Receptor Pathway in Rats. *Evid Based Complement Alternat Med* 2011: 248481, 2011.
61. **van Norren K, Kegler D, Argiles JM, Luiking Y, Gorselink M, Laviano A, Arts K, Faber J, Jansen H, van der Beek EM, van Helvoort A.** Dietary supplementation with a specific combination of high protein, leucine, and fish oil improves muscle function and daily activity in tumour-bearing cachectic mice. *Br J Cancer* 100: 713–722, 2009.
62. **Yamamoto Y, Ueta Y, Yamashita H, Asayama K, Shirahata A.** Expressions of the prepro-orexin and orexin type 2 receptor genes in obese rat. *Peptides* 23: 1689–1696, 2002.
63. **Yanagihara K, Takigahira M, Mihara K, Kubo T, Morimoto C, Morita Y, Terawaki K, Uezono Y, Seyama T.** Inhibitory effects of isoflavones on tumor growth and cachexia in newly established cachectic mouse models carrying human stomach cancers. *Nutr Cancer* 65: 578–589, 2013.
64. **Yanai M, Mochiki E, Ogawa A, Morita H, Toyomasu Y, Ogata K, Tabe Y, Ando H, Ohno T, Asao T, Aomori T, Fujita Y, Kuwano H.** Intragastric administration of rikkunshito stimulates upper gastrointestinal motility and gastric emptying in conscious dogs. *J Gastroenterol* 48: 611–619, 2013.
65. **Yoshimura M, Matsuura T, Ohkubo J, Ohno M, Maruyama T, Ishikura T, Hashimoto H, Kakuma T, Yoshimatsu H, Terawaki K, Uezono Y, Ueta Y.** The gene expression of the hypothalamic feeding-regulating peptides in cisplatin-induced anorexic rats. *Peptides* 46: 13–19, 2013.
66. **Zaki MH, Nemeth JA, Trikha M.** CNTO 328, a monoclonal antibody to IL-6, inhibits human tumor-induced cachexia in nude mice. *Int J Cancer* 111: 592–595, 2004.

The Endocannabinoid Anandamide Inhibits Voltage-Gated Sodium Channels $Na_v1.2$, $Na_v1.6$, $Na_v1.7$, and $Na_v1.8$ in *Xenopus* Oocytes

Dan Okura, MD,* Takafumi Horishita, MD, PhD,* Susumu Ueno, MD, PhD,† Nobuyuki Yanagihara, PhD,‡ Yuka Sudo, PhD,§ Yasuhito Uezono, MD, PhD,‖ and Takeyoshi Sata, MD, PhD*

BACKGROUND: Anandamide is an endocannabinoid that regulates multiple physiological functions by pharmacological actions, in a manner similar to marijuana. Recently, much attention has been paid to the analgesic effect of endocannabinoids in terms of identifying new pharmacotherapies for refractory pain management, but the mechanisms of the analgesic effects of anandamide are still obscure. Voltage-gated sodium channels are believed to play important roles in inflammatory and neuropathic pain. We investigated the effects of anandamide on 4 neuronal sodium channel α subunits, $Na_v1.2$, $Na_v1.6$, $Na_v1.7$, and $Na_v1.8$, to explore the mechanisms underlying the antinociceptive effects of anandamide.

METHODS: We studied the effects of anandamide on $Na_v1.2$, $Na_v1.6$, $Na_v1.7$, and $Na_v1.8$ α subunits with β_1 subunits by using whole-cell, 2-electrode, voltage-clamp techniques in *Xenopus* oocytes.

RESULTS: Anandamide inhibited sodium currents of all subunits at a holding potential causing half-maximal current ($V_{1/2}$) in a concentration-dependent manner. The half-maximal inhibitory concentration values for $Na_v1.2$, $Na_v1.6$, $Na_v1.7$, and $Na_v1.8$ were 17, 12, 27, and 40 μmol/L, respectively, indicating an inhibitory effect on $Na_v1.6$, which showed the highest potency. Anandamide raised the depolarizing shift of the activation curve as well as the hyperpolarizing shift of the inactivation curve in all α subunits, suggesting that sodium current inhibition was due to decreased activation and increased inactivation. Moreover, anandamide showed a use-dependent block in $Na_v1.2$, $Na_v1.6$, and $Na_v1.7$ but not $Na_v1.8$.

CONCLUSION: Anandamide inhibited the function of α subunits in neuronal sodium channels $Na_v1.2$, $Na_v1.6$, $Na_v1.7$, and $Na_v1.8$. These results help clarify the mechanisms of the analgesic effects of anandamide. (Anesth Analg 2014;118:554–62)

Cannabis has been used as a pleasure-inducing drug and traditional medicine for thousands of years, and since the 2 cannabinoid receptors CB_1[1,2] and CB_2[3] were identified, the endocannabinoid signaling system has been a focus of medical research and has been considered a potential therapeutic target.[4] Endocannabinoids mimic the pharmacological actions of the psychoactive principle agent in marijuana, Δ^9-tetrahydrocannabinol, and regulate multiple physiological functions, such as analgesia, regulation of food intake, immunomodulation, inflammation, addictive behavior, epilepsy, and others.[5]

Anandamide, the ethanolamide of arachidonic acid, was the first endocannabinoid isolated from the brain[6]; it acts as a partial agonist on CB_1 receptors, with a lesser effect on CB_2 receptors.[7] Several groups have shown an analgesic effect of exogenous anandamide through the CB_1 receptor in acute,[8–10] persistent inflammatory,[11–13] and neuropathic pain models.[14,15] CB_1 receptors are distributed throughout the pain pathways of the central nervous system (CNS), including the periaqueductal gray, amygdala, and spinal trigeminal tract,[16,17] and the peripheral nervous system including the dorsal root ganglion (DRG),[18] suggesting an analgesic effect of anandamide via CB_1 receptors. However, anandamide may also act on other ion channels consisting of pain signaling pathways, including voltage-gated Ca^{2+} channels, TASK1 channels, 5-HT_3 receptor, rectifying K^+ channels, and N-methyl-D-aspartate receptors[19–24]; thus, the mechanisms of the analgesic effects of anandamide remain unclear.

Voltage-gated sodium channels play an essential role in action potential initiation and propagation in excitable nerve and muscle cells. Nine distinct pore-forming α subunits ($Na_v1.1$–$Na_v1.9$), which are associated with auxiliary β subunits, have been identified,[25,26] and each has a different pattern of development and localization as well as distinct physiological and pathophysiological roles. Sodium channel α subunits expressed in DRG ($Na_v1.7$, $Na_v1.8$, $Na_v1.9$) are believed to play crucial roles in inflammatory and neuropathic pain and are considered potential targets of these conditions.[27–30] Previous studies have shown that anandamide inhibits sodium channel function in the brain through the inhibition of veratridine-dependent depolarization of synaptosomes[31] and suppresses tetrodotoxin-sensitive (TTX-S) and tetrodotoxin-resistant (TTX-R) sodium currents in rat

From the *Department of Anesthesiology, School of Medicine; †Department of Occupational Toxicology, Institute of Industrial Ecological Sciences, University of Occupational and Environmental Health, ‡Department of Pharmacology, School of Medicine, University of Occupational and Environmental Health, Fukuoka; §Department of Molecular Pathology & Metabolic Disease, Faculty of Pharmaceutical Sciences, Tokyo university of Science, Chiba; and ‖Cancer Pathophysiology Division, National Cancer Center Research Institute, Tokyo, Japan.

Accepted for publication November 15, 2013.

Funding: This study was supported by a Grant-in-Aid for Scientific Research from the Ministry of Education, Culture, Sports, Science and Technology, 24592369 (to T.H.).

The authors declare no conflicts of interest.

Reprints will not be available from the authors.

Address correspondence to Takafumi Horishita, MD, PhD, Department of Anesthesiology, School of Medicine, University of Occupational and Environmental Health, 1-1 Iseigaoka, Yahatanishiku, Kitakyushu, Fukuoka 807–8555, Japan. Address e-mail to thori@med.uoeh-u.ac.jp.

DOI: 10.1213/ANE.0000000000000070

DRG neurons.[32] These results suggest that sodium channels are potential targets for anandamide. However, the precise mechanisms of anandamide on each α subunit are still unknown. It is of great importance to clarify these mechanisms because each α subunit has a difference of 20% to 50% in amino acid sequence in the transmembrane and extracellular domains and therefore has different physiological functions. Here, we explored the effects of anandamide on several sodium channel α subunits, including $Na_v1.2$, that is expressed primarily in the CNS; $Na_v1.6$ that is expressed in the CNS and DRG neurons; and $Na_v1.7$ and $Na_v1.8$ that are expressed in DRG neurons.

METHODS

This study was approved by the Animal Research Committee of the University of Occupational and Environmental Health.

Materials

Adult female *Xenopus laevis* frogs were obtained from Kyudo Co., Ltd. (Saga, Japan). Anandamide was purchased from Sigma-Aldrich (St. Louis, MO). Rat $Na_v1.2$ α subunit cDNA was a gift from Dr. W. A. Catterall (University of Washington, Seattle, WA). Rat $Na_v1.6$ α subunit cDNA was a gift from Dr. A. L. Goldin (University of California, Irvine, CA). Rat $Na_v1.7$ α subunit cDNA was a gift from G. Mandel (Oregon Health and Science University, Portland, OR). Rat $Na_v1.8$ α subunit cDNA was a gift from Dr. A. N. Akopian (University of Texas Health Science Center, San Antonio, TX), and human β_1 subunit cDNA was a gift from Dr. A. L. George (Vanderbilt University, Nashville, TN).

cRNA Preparation and Oocyte Injection

After linearization of cDNA with *ClaI* ($Na_v1.2$ α subunit), *NotI* ($Na_v1.6$, 1.7 α subunit), *XbaI* ($Na_v1.8$ α subunit), and *EcoRI* (β_1 subunit), cRNAs were transcribed by using SP6 (1.8 α, β_1 subunit) or T7 ($Na_v1.2$, 1.6 1.7 α subunit) RNA polymerase from the mMESSAGE mMACHINE kit (Ambion, Austin, TX). Preparation of *X. laevis* oocytes and cRNA microinjection were performed as described previously.[33] Briefly, stage IV to VI oocytes were manually isolated from a removed portion of ovary. Next, oocytes were treated with collagenase (0.5 mg/mL) for 10 minutes and placed in modified Barth's solution (88 mmol/L NaCl, 1 mmol/L KCl, 2.4 mmol/L $NaHCO_3$, 10 mmol/L HEPES, 0.82 mmol/L $MgSO_4$, 0.33 mmol/L $Ca(NO_3)_2$, and 0.91 mmol/L $CaCl_2$, adjusted to pH 7.5), supplemented with 10,000 U penicillin, 50 mg gentamicin, 90 mg theophylline, and 220 mg sodium pyruvate per liter (incubation medium). Na_v α subunit cRNAs were coinjected with β_1 subunit cRNA at a ratio of 1:10 (total volume was 20–40 ng/50 nL) into *Xenopus* oocytes (all α subunits were coinjected with the β_1 subunit). Injected oocytes were incubated at 19°C in incubation medium, and 2 to 6 days after injection, the cells were used for electrophysiological recordings.

Electrophysiological Recordings

All electrical recordings were performed at room temperature (23°C). Oocytes were placed in a 100 μL recording chamber and perfused at 2 mL/min with Frog Ringer's solution containing 115 mmol/L NaCl, 2.5 mmol/L KCl, 10 mmol/L HEPES, 1.8 mmol/L $CaCl_2$, pH 7.2, by using a peristaltic pump (World Precision Instruments Inc., Sarasota, FL). Recording electrodes were prepared with borosilicate glass by using a puller (PP-830, Narishige group company, Tokyo, Japan), and microelectrodes were filled with 3 mol KCl/0.5% low-melting-point agarose with resistances between 0.3 and 0.5 MΩ. The whole-cell voltage clamp was achieved through these 2 electrodes by using a Warner Instruments model OC-725C (Warner, Hamden, CT). Currents were recorded and analyzed by using pCLAMP 7.0 software (Axon Instruments, Foster City, CA), and the amplitude of expressed sodium currents was typically 2 to 15 μA. Transients and leak currents were subtracted by using the P/N procedure. Anandamide stocks were prepared in dimethylsulphoxide (DMSO) and diluted in Frog Ringer's solution to a final DMSO concentration not exceeding 0.05%. Anandamide was then perfused for 5 to 10 minutes to reach equilibrium.

The voltage dependence of activation was determined by using 50-millisecond depolarizing pulses from a holding potential causing maximal current, V_{max} (–90 mV for $Na_v1.2$ and $Na_v1.6$ or –100 mV for $Na_v1.7$ and $Na_v1.8$), and from a holding potential causing half-maximal current, $V_{1/2}$ (from approximately –40 mV to –70 mV) to 50 mV in 10 mV increments. Normalized activation curves were fitted to the Boltzmann equation: $G/G_{max} = 1/(1 + \exp(V_{1/2} - V)/k)$, where G is the voltage-dependent sodium conductance, G_{max} is the maximal sodium conductance, G/G_{max} is the normalized fractional conductance, $V_{1/2}$ is the potential at which activation is half maximal, and k is the slope factor. The G value for each oocyte was calculated by using the formula $G = I/(Vt - Vr)$, where I is the peak sodium current, Vt is the test potential and Vr is the reversal potential. The Vr for each oocyte was estimated by extrapolating the linear ascending segment of the current voltage relationship (I–V) curve to the voltage axis. To measure steady-state inactivation, currents were elicited by a 50-millisecond test pulse to –20 mV for $Na_v1.2$ and $Na_v1.6$ or –10 mV for $Na_v1.7$ or +10 mV for $Na_v1.8$ after 200 milliseconds (500 milliseconds for only $Na_v1.8$) prepulses ranging from –140 mV to 0 mV in 10 mV increments from a holding potential of V_{max}. Steady-state inactivation curves were fitted to the Boltzmann equation: $I/I_{max} = 1/(1 + \exp(V_{1/2} - V)/k)$, where I_{max} is the maximal sodium current, I/I_{max} is the normalized current, $V_{1/2}$ is the voltage of half-maximal inactivation, and k is the slope factor. To investigate a use-dependent sodium channel block of anandamide, currents were elicited at 10 Hz by a 20-millisecond depolarizing pulse of –20 mV for $Na_v1.2$ and $Na_v1.6$ or –10 mV for $Na_v1.7$ or +10 mV for $Na_v1.8$ from a $V_{1/2}$ holding potential in both the absence and presence of 30 μmol/L anandamide. Peak currents were measured and normalized to the first pulse and plotted against the pulse number. Data were fitted to the monoexponential equation $I_{Na} = \exp(-\tau_{use} \cdot n) + C$, where n is pulse number, C is the plateau I_{Na}, and τ_{use} is the time constant of use-dependent decay.

Data Analysis

All values are presented as the mean ± SEM (n = 5–8). The n values refer to the number of oocytes examined. Each experiment was performed with oocytes from at least 2 frogs.

Control sodium current recorded in absence of anandamide was assigned a value of 100%. Data were statistically evaluated by paired *t* test by using GraphPad Prism software (GraphPad Software, Inc., San Diego, CA). Hill slope and half-maximal inhibitory concentration values were also calculated by using this software.

RESULTS

Effects of Anandamide on Peak Na+ Inward Currents

Currents were elicited by using a 50-millisecond depolarizing pulse to –20 mV for $Na_v1.2$ and $Na_v1.6$ or –10 mV for $Na_v1.7$ or +10 mV for $Na_v1.8$ applied every 10 seconds from V_{max} or $V_{1/2}$ holding potential in both the absence and presence of 10 μmol/L anandamide (Fig. 1); anandamide was applied for 10 minutes. Anandamide inhibited the peak I_{Na} induced by all α subunits more potently at $V_{1/2}$ than V_{max}. Anandamide reduced the peak I_{Na} induced by $Na_v1.2$, $Na_v1.6$, $Na_v1.7$, and $Na_v1.8$ by 46 ± 4, 49 ± 3, 37 ± 2, and 27 ± 2 at $V_{1/2}$, respectively, and 7 ± 2, 6 ± 1, 9 ± 1, and 21 ± 5% at V_{max}, respectively (Fig. 2). Inhibition of anandamide at $V_{1/2}$ was statistically significant in all α subunits, but those at V_{max} were not statistically significant except for the suppression in $Na_v1.8$ by paired *t* test. Because suppression at $V_{1/2}$ was potent, we examined the concentration-response relation for anandamide inhibition of the peak I_{Na} induced by $Na_v1.2$, $Na_v1.6$, $Na_v1.7$, and $Na_v1.8$ at $V_{1/2}$ holding potential (Fig. 3). The peak current amplitude in the presence of anandamide was normalized to that in the control, and the effects of anandamide were expressed as percentages of the control. Nonlinear regression analyses of the dose-response curves yielded half-maximal inhibitory concentration values and Hill slopes of 17 ± 3 μmol/L and 0.74 ± 0.04 for $Na_v1.2$, 12 ± 1 μmol/L and 0.79 ± 0.08 for $Na_v1.6$, 27 ± 3 μmol/L and 0.52 ± 0.06 for $Na_v1.7$, 40 ± 14 μmol/L and 0.71 ± 0.10 for $Na_v1.8$, respectively (Fig. 3).

Effects of Anandamide on Sodium Current Activation

We examined the effects of anandamide on 4 α subunits of sodium current activation. Voltage dependence of activation was determined by using 50-millisecond depolarizing pulses from a holding potential of V_{max} to 50 mV in 10 mV increments or from a holding potential of $V_{1/2}$ to 50 mV in 10 mV increments for $Na_v1.2$, $Na_v1.6$, $Na_v1.7$, and $Na_v1.8$. Activation curves were derived from the I-V curves (see Methods); anandamide (30 μmol/L) was applied for 5 minutes. The peak I_{Na} was reduced by anandamide at V_{max} and $V_{1/2}$ holding potentials with all subunits (Fig. 4). Anandamide shifted the midpoint of steady-state activation ($V_{1/2}$) in a depolarizing direction at both holding potentials for all subunits (Fig. 5). These shifts were small (1.9–3.8 mV) but statistically significant (Table 1).

Effects of Anandamide on Sodium Current Inactivation

The effect of anandamide on steady-state inactivation was also investigated. Currents were elicited by a 50-millisecond test pulse to –20 mV for $Na_v1.2$ and $Na_v1.6$ or –10 mV for $Na_v1.7$ or +10 mV for $Na_v1.8$ after 200 millis econds(500 milliseconds for only $Na_v1.8$) prepulses ranging from –140 mV to 0 mV in 10 mV increments from a holding potential of V_{max}. Steady-state inactivation curves were fitted to the Boltzmann equation (see Methods); anandamide (30 μmol/L) was applied for 5 minutes. Anandamide significantly shifted the midpoint of steady-state inactivation ($V_{1/2}$) in the hyperpolarizing direction by 5.2, 5.0, 4.1, and 6.3 mV in $Na_v1.2$, $Na_v1.6$, $Na_v1.7$, and $Na_v1.8$, respectively (Fig. 6, Table 1).

Use-Dependent Block of Sodium Currents by Anandamide

We investigated the use-dependent block of sodium currents by anandamide. Currents were elicited at 10 Hz by a 20-millisecond depolarizing pulse of –20 mV for $Na_v1.2$ and $Na_v1.6$ or –10 mV for $Na_v1.7$ or +10 mV for $Na_v1.8$ from a $V_{1/2}$ holding potential in both the absence and presence of 30 μmol/L anandamide. Peak currents were measured and normalized to the first pulse and plotted against the pulse number (Fig. 7, A–D). Data were fitted by the monoexponential equation (see Methods); anandamide was applied for 5 minutes. Anandamide significantly reduced the plateau I_{Na} amplitude of $Na_v1.2$, $Na_v1.6$, and $Na_v1.7$ from 0.74 ± 0.02 to 0.66 ± 0.03, 0.88 ± 0.01 to 0.66 ± 0.02, and 0.73 ±

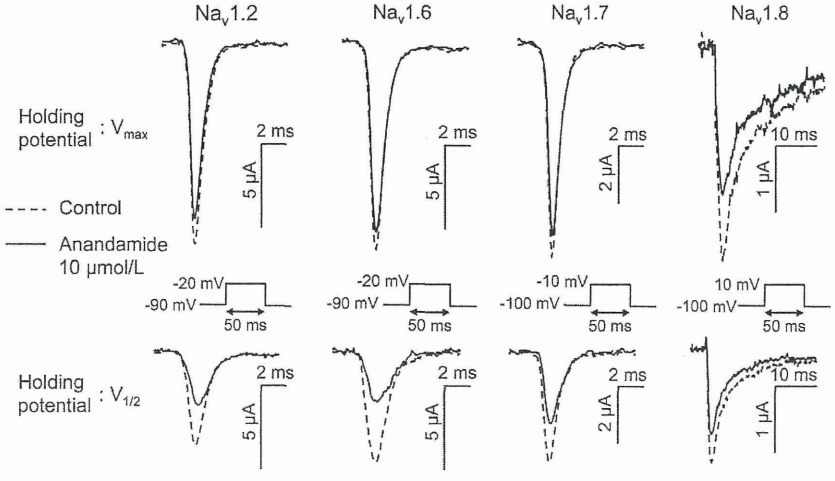

Figure 1. Inhibitory effects of anandamide on peak sodium inward currents in *Xenopus* oocytes expressing $Na_v1.2$, $Na_v1.6$, $Na_v1.7$, and $Na_v1.8$ α subunits with β_1 subunits at 2 holding potentials. Representative traces are shown. Sodium currents were evoked by 50-millisecond depolarizing pulses to –20 mV for $Na_v1.2$ and $Na_v1.6$ or –10 mV for $Na_v1.7$ or +10 mV for $Na_v1.8$ from V_{max} holding potential (upper panel) or $V_{1/2}$ holding potential (lower panel) in both the absence and presence of 10 μmol/L anandamide; anandamide was applied for 10 minutes.

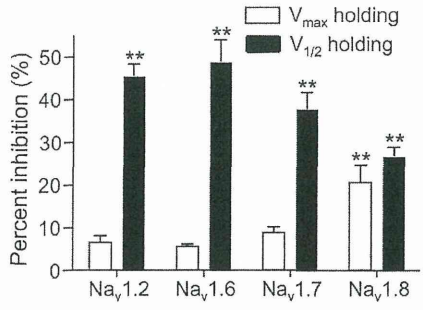

Figure 2. Inhibitory effects of anandamide on peak sodium inward currents in *Xenopus* oocytes expressing $Na_v1.2$, $Na_v1.6$, $Na_v1.7$, and $Na_v1.8$ α subunits with β_1 subunits at 2 holding potentials. Percent inhibition of sodium current of anandamide was calculated. Open columns represent the effect at V_{max} holding potential, and closed columns indicate the effect at $V_{1/2}$ holding potential. Anandamide inhibited the peak I_{Na} induced by $Na_v1.2$, $Na_v1.6$, $Na_v1.7$, and $Na_v1.8$ by 46 ± 4, 49 ± 3, 37 ± 2, and 27 ± 2 at $V_{1/2}$, respectively, and 7 ± 2, 6 ± 1, 9 ± 1, and 21 ± 5% at V_{max}, respectively. Data are represented as the mean ± SEM (n = 5–7). $^{**}P < 0.01$, compared with the control (based on paired t test).

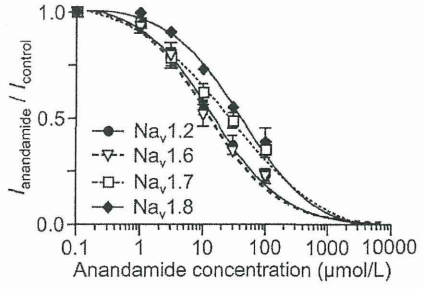

Figure 3. Concentration-response curves for anandamide suppression of sodium currents elicited by 50-millisecond depolarizing pulses to –20 mV for $Na_v1.2$ and $Na_v1.6$ or –10 mV for $Na_v1.7$ or +10 mV for $Na_v1.8$ from $V_{1/2}$ holding potential. The peak current amplitude in the presence of anandamide was normalized to that in the control, and the effects of anandamide are expressed as percentages of the control. Half-maximal inhibitory concentration values and Hill slopes were 17 ± 3 μmol/L and 0.74 ± 0.04 for $Na_v1.2$, 12 ± 1 μmol/L and 0.79 ± 0.08 for $Na_v1.6$, 27 ± 3 μmol/L and 0.52 ± 0.06 for $Na_v1.7$, and 40 ± 14 μmol/L and 0.71 ± 0.10 for $Na_v1.8$, respectively. Data are represented as the mean ± SEM (n = 5–8). Data were fit to the Hill slope equation to give the half-maximal inhibitory concentration values and Hill slopes. Half-maximal inhibitory concentration values and Hill slopes were calculated by using GraphPad Prism.

0.03 to 0.57 ± 0.04, respectively (Fig. 7E), demonstrating a use-dependent block, whereas anandamide did not reduce the plateau I_{Na} amplitude of $Na_v1.8$ (from 0.86 ± 0.03 to 0.84 ± 0.04).

DISCUSSION

In the present study, we demonstrated that anandamide suppresses the $Na_v1.2$, $Na_v1.6$, $Na_v1.7$, and $Na_v1.8$ α subunits in a concentration-dependent manner. half-maximal inhibitory concentration values ranged from 12 μmol/L ($Na_v1.6$) to 40 μmol/L ($Na_v1.8$). Wiley et al.[34] have reported that IV administration of anandamide produce a dose-dependent antinociceptive effect in the tail-flick test with mice, and the 50% effective dose (ED_{50}) of that was 15 mg/kg. They also have shown that the plasma concentration of anandamide was 4.96 μg/mL (14.3 μmol/L) when 10 mg/kg of anandamide was administered, suggesting that half-maximal inhibitory concentration values used in the present study are pharmacologically relevant and are close to the plasma concentration exhibiting an antinociceptive effect by anandamide. We also demonstrated that anandamide has more potent inhibitory effects on sodium currents at $V_{1/2}$ holding potential (inactivated state) than at V_{max} holding potential (resting state) in a manner similar to that of local anesthetics on sodium channels. Therefore, the analgesic effects of anandamide may be mediated through sodium channel blockade. The present results are partially consistent with previous reports that anandamide suppresses TTX-S veratridine-dependent depolarization of synaptosomes, the binding of batrachotoxin to sodium channels, and TTX-S sustained repetitive firing in cortical neurons[31] and inhibits TTX-S and TTX-R sodium currents in a concentration-dependent manner in rat DRG neurons.[32] However, their precise mechanisms of anandamide on several sodium channel α subunits have not yet been investigated. Considering that $Na_v1.6$ was distributed in both CNS and DRG neurons, and that $Na_v1.8$ was distributed in DRG neurons, our results are consistent with a previous study showing that anandamide inhibited sodium currents with half-maximal inhibitory concentration values of 5.4 μmol/L for the TTX-S current and 38 μmol/L for the TTX-R current in DRG neurons,[32] suggesting that TTX-S and TTX-R currents in DRG neurons may represent $Na_v1.6$ and $Na_v1.8$ currents, respectively. Because $Na_v1.6$ is expressed in both the brain and DRG, and anandamide suppressed $Na_v1.6$ function most potently among the 4 α subunits, the effect of anandamide on $Na_v1.6$ may be the most important.

The effects of anandamide on channel gating, including activation and inactivation, demonstrated common characteristics among the 4 α subunits we studied. Anandamide shifted the midpoint of steady-state activation ($V_{1/2}$) in a depolarizing direction at both $V_{1/2}$ and V_{max} holding potentials for all α subunits, and the shifts were significant, although the shifts were small (approximately 4 mV). Anandamide also significantly shifted the midpoint of steady-state inactivation ($V_{1/2}$) in the hyperpolarizing direction (approximately 7 mV) for all α subunits. These results suggest that both inhibition of activation and the enhancement of inactivation are common mechanisms of sodium current inhibition by anandamide for $Na_v1.2$, $Na_v1.6$, $Na_v1.7$, and $Na_v1.8$. A combination of effects on both activation and inactivation might produce sufficient effects to suppress sodium currents although each effect is small. Inhibition by anandamide at V_{max} holding potential for $Na_v1.2$, $Na_v1.6$, and $Na_v1.7$ was small and not significant, whereas that for $Na_v1.8$ was significant (Fig. 1), indicating that resting-channel block is one of the important mechanisms of anandamide inhibition for only $Na_v1.8$. Anandamide exhibited use-dependent block with repetitive stimuli for $Na_v1.2$, $Na_v1.6$, and $Na_v1.7$ but not $Na_v1.8$. The presence of use-dependent block by anandamide suggests the possibility of open-channel block and the ability to slow the recovery time from blocks that are seen with amitriptyline.[35] Sodium channel blockers such as local anesthetics, tricyclic antidepressants, and volatile anesthetics have been shown to shift the voltage dependence of steady-state inactivation with no effect on

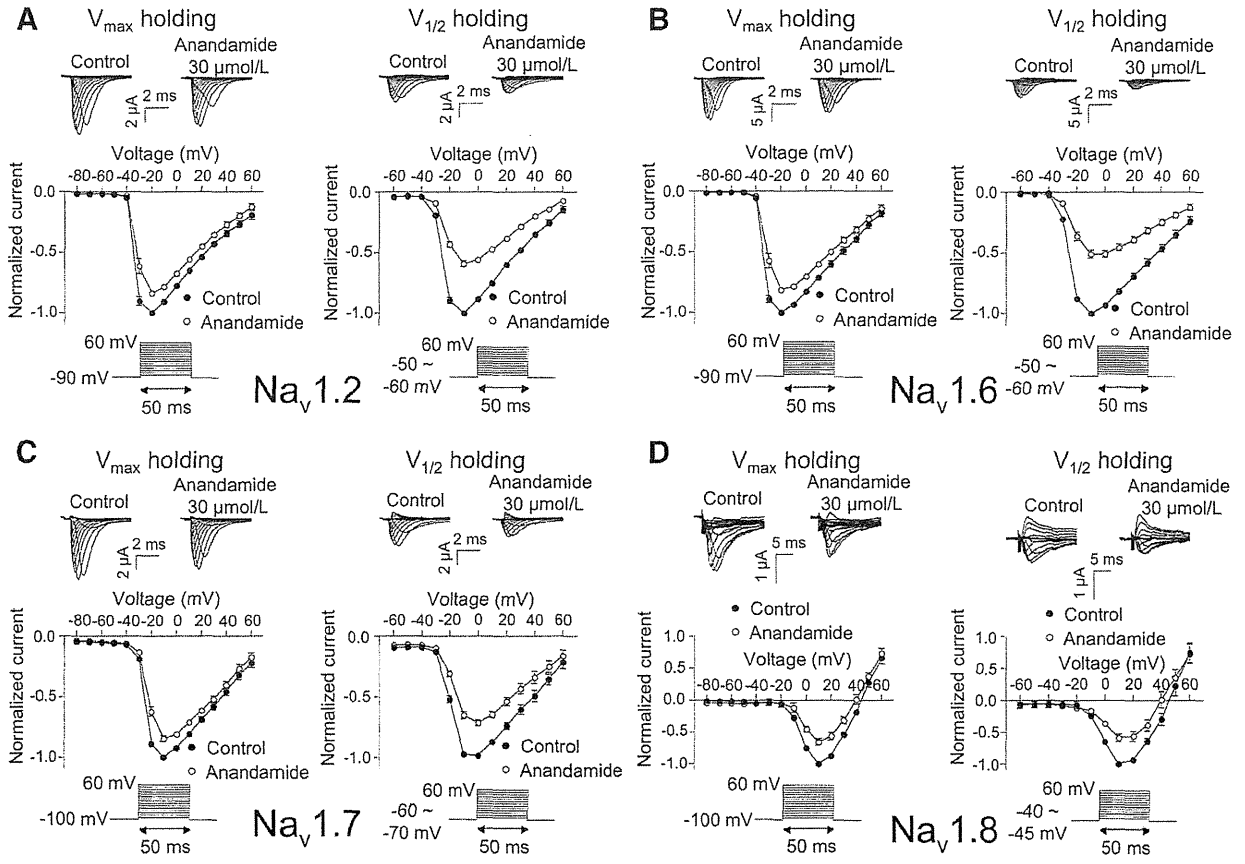

Figure 4. Effects of anandamide on I-V curves of sodium currents in oocytes expressing $Na_v1.2$ (A), $Na_v1.6$ (B), $Na_v1.7$ (C), and $Na_v1.8$ (D) α subunits with β_1 subunits. Currents were elicited by using 50-millisecond depolarizing steps between –80 and 60 mV in 10 mV increments from a V_{max} holding potential (left panel) and elicited by using 50-millisecond depolarizing steps between –60 and 60 mV in 10 mV increments from a $V_{1/2}$ holding potential (right panel); anandamide (30 μmol/L) was applied for 5 minutes; upper panel, representative I_{Na} traces from oocytes expressing $Na_v1.2$, $Na_v1.6$, $Na_v1.7$, and $Na_v1.8$ with β_1 subunits in both the absence and presence of 30 μmol/L anandamide; lower panel, effects of anandamide on representative I-V curves elicited from V_{max} holding potential (left panel) and $V_{1/2}$ holding potential (right panel) (closed circles, control; open circles, anandamide). Peak currents were normalized to the maximal currents observed from –20 to +10 mV. Data are represented as the mean ± SEM (n = 5–8).

activation and exhibit use-dependent block.[35–39] Our results show that anandamide shows a negative shift in the voltage dependence of inactivation and use-dependent block except for $Na_v1.8$ that are seen with other sodium channel blockers yet also shifts the steady-state activation in a depolarizing direction, suggesting that it may have different binding sites or allosteric conformational mechanisms for these sodium channel antagonists. Moreover, a resting-channel block, not an open-channel block, for $Na_v1.8$ may be a key for exploring the mechanism of sodium channel inhibition by anandamide in detail.

Several groups have evaluated antinociception by exogenous anandamide via CB_1 receptors.[8–10] Indeed, a recent review has shown that activation of both CB_1 and CB_2 receptors reduces nociceptive processing in acute and chronic animal models of pain.[40] Alternatively, other investigators have suggested that anandamide produces antinociception through a CB_1-independent mechanism. For example, anandamide antinociception is not blocked by pretreatment with the selective CB_1 antagonist SR141716A.[41] Rapid metabolism of anandamide to arachidonic acid has been shown to be one of the reasons for the failure of SR141716A to antagonize the effects of anandamide; in experiments, the ability of SR141716A to reverse anandamide antinociception was improved (but not completely) when anandamide metabolism to arachidonic acid was inhibited with coadministration of an amidase inhibitor, phenylmethylsulfonyl fluoride.[42] That study also demonstrated that cyclooxygenase did not alter the effects of anandamide, whereas it blocked the effects of arachidonic acid, suggesting a pain-inhibitory effect of anandamide by noncannabinoid mechanisms. Another recent study suggested that anandamide induced antinociception by stimulating endogenous norepinephrine release that activated peripheral adrenoceptors inducing antinociception, although whether the effect was caused through cannabinoid receptors remains unknown.[43]

This study indicates that sodium channel inhibition by anandamide is independent of signaling through cannabinoid receptors, because in recombinant experiments such as our present examination, the effects on channels or receptors can be excluded except for that expressed in membranes. Previous reports also indicate a direct effect of anandamide on sodium channels by demonstrating that sodium channel-related activities by anandamide in the brain may be independent of

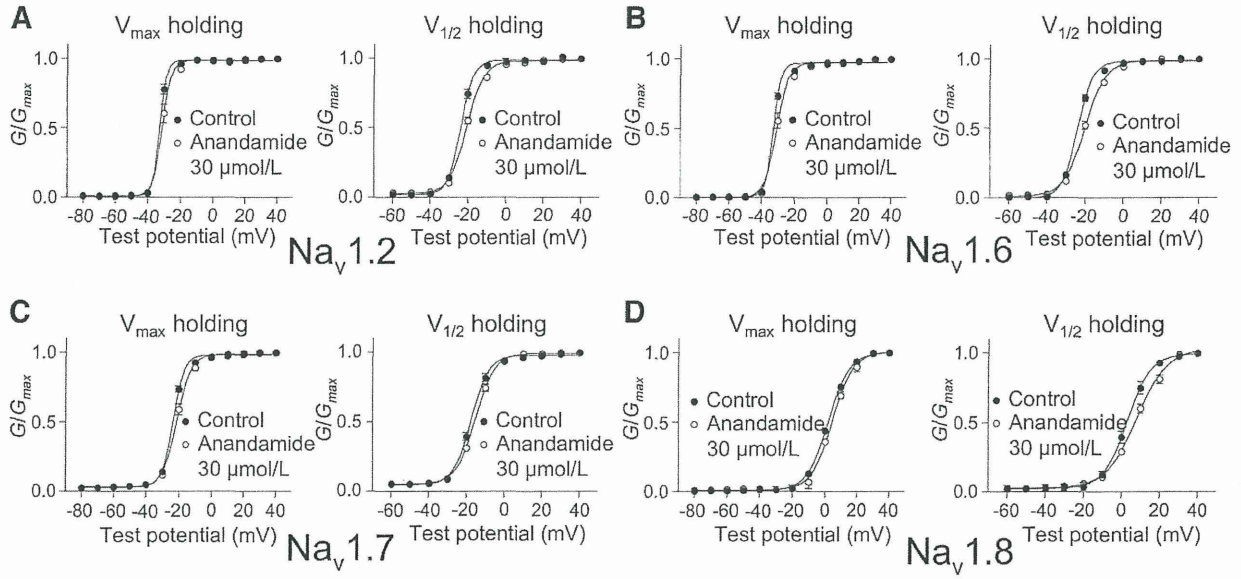

Figure 5. Effects of anandamide on channel activation in oocytes expressing $Na_v1.2$ (A), $Na_v1.6$ (B), $Na_v1.7$ (C), and $Na_v1.8$ (D) α subunits with β_1 subunits from V_{max} holding potential (left panels) or $V_{1/2}$ holding potential (right panels). Closed circles represent control; open circles indicate the effect of anandamide. Data are expressed as the mean ± SEM (n = 5–8). Activation curves were fitted to the Boltzmann equation; $V_{1/2}$ is shown in Table 1.

Table 1. Effects of Anandamide on Activation and Inactivation in Oocytes Expressing $Na_v1.2$, $Na_v1.6$, $Na_v1.7$, and $Na_v1.8$ α Subunits with β_1 Subunits

	$V_{1/2}$ (mV)					
	Holding V_{max}			Holding $V_{1/2}$		
	Control	Anandamide	Shift	Control	Anandamide	Shift
Activation						
$Na_v1.2$	−32.7 ± 0.3	−30.8 ± 0.7*	+1.9	−23.6 ± 0.6	−20.4 ± 0.6**	+3.2
$Na_v1.6$	−32.6 ± 0.3	−30.5 ± 0.7*	+2.1	−23.8 ± 0.5	−20.0 ± 0.6**	+3.8
$Na_v1.7$	−23.4 ± 0.4	−21.0 ± 0.8*	+2.4	−17.3 ± 0.7	−15.0 ± 0.7*	+2.3
$Na_v1.8$	2.2 ± 0.2	4.8 ± 0.8*	+2.6	3.3 ± 1.0	8.4 ± 1.1*	+3.3
Inactivation						
$Na_v1.2$	−51.4 ± 0.7	−56.6 ± 0.8**	−5.2			
$Na_v1.6$	−53.5 ± 0.8	−58.5 ± 1.0**	−5.0			
$Na_v1.7$	−64.3 ± 0.7	−68.4 ± 0.6**	−4.1			
$Na_v1.8$	−50.7 ± 1.4	−57.0 ± 1.9*	−6.3			

*P < 0.05.
**P < 0.01, compared with control (paired t test) (mean ± SEM; n = 5–7).

the presence of AM 251 (a CB_1 antagonist),[31] AM 251, AM 630 (a CB_2 antagonist) and capsazepine (a vanilloid receptor type 1 antagonist) do not interfere with anandamide suppression of sodium currents in DRG.[32] Therefore, we believe that the effects of anandamide on $Na_v1.2$, $Na_v1.6$, $Na_v1.7$, and $Na_v1.8$ α subunits are direct. Taken together, to the best of our knowledge, this is the first direct evidence to demonstrate the inhibitory effects and its mechanisms on neuronal sodium channel α subunits in recombinant experiment systems.

Several sodium channel α subunits are believed to be involved in the pathogenesis of inflammatory and neuropathic pain. Mutations in $Na_v1.7$ have been linked to inherited pain syndromes, including inherited erythromelalgia, that is characterized by episodes of burning pain, erythema, mild swelling in the hands and feet,[44] and paroxysmal extreme pain disorder (PEPD), which is characterized by severe rectal, ocular, and mandibular pain.[45] Recently, anandamide has been reported to inhibit resurgent current of wild-type $Na_v1.7$ and the PEPD mutants expressed in transfected human embryonic kidney 293 cells, and this inhibition was suggested as a therapeutic target for PEPD patients.[46] $Na_v1.8$ has demonstrated its ability to carry most current underlying the upstroke of the action potential in nociceptive neurons,[47] and the use of $Na_v1.8$ knockdown rats after antisense oligodeoxynucleotide treatment has demonstrated a role for $Na_v1.8$ in inflammatory pain,[48] whereas $Na_v1.8$ expression has been reported to increase in nerves proximal to injury sites in patients with chronic neuropathic pain.[49] In an infraorbital nerve injury model of rats, the level of $Na_v1.6$ protein was significantly increased proximal to the lesion site, suggesting a role of $Na_v1.6$ in neuropathic pain conditions.[50] However, these α subunits highly expressed in normal DRG have been reported to show diverse expression in DRG of inflammatory and neuropathic pain models. $Na_v1.7$ mRNA and protein increased in DRG after peripheral inflammation induced by

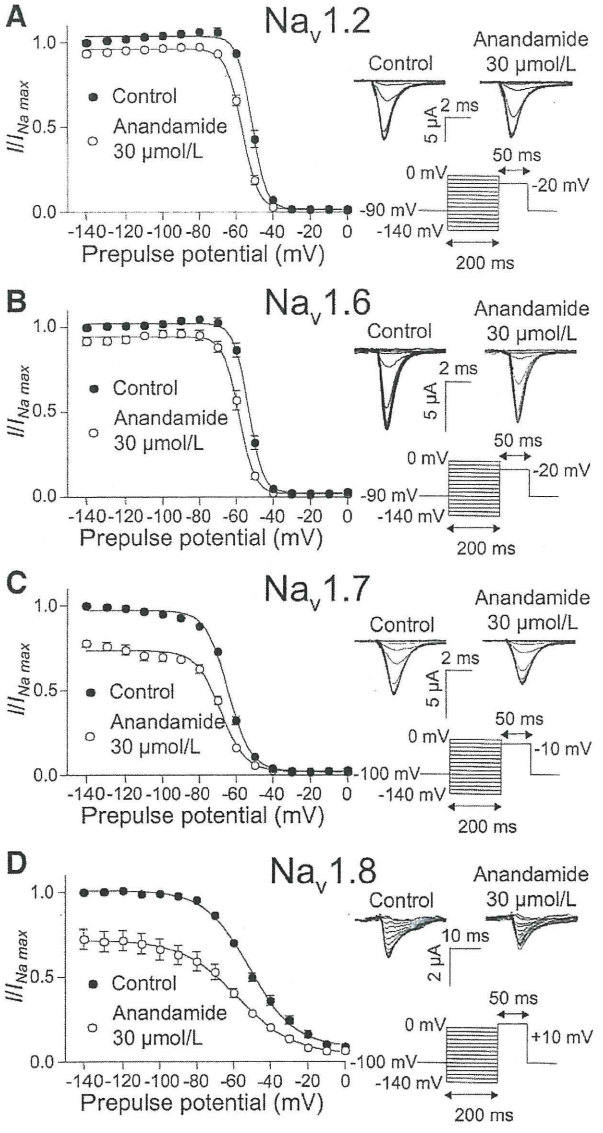

Figure 6. Effects of anandamide on inactivation curves in oocytes expressing $Na_v1.2$ (A), $Na_v1.6$ (B), $Na_v1.7$ (C), and $Na_v1.8$ (D) α subunits with β_1 subunits. Currents were elicited by a 50-millisecond test pulse to –20 mV for $Na_v1.2$ and $Na_v1.6$ or –10 mV for $Na_v1.7$ or +10 mV for $Na_v1.8$ after 200-millisecond (500-millisecond for only $Na_v1.8$) prepulses ranging from –140 mV to 0 mV in 10 mV increments from a holding potential of V_{max}; anandamide (30 μmol/L) was applied for 5 minutes; right panel, representative I_{Na} traces in both the absence and presence of anandamide; left panel, effects of anandamide on inactivation curves (closed circles, control; open circles, anandamide). Steady-state inactivation curves were fitted to the Boltzmann equation, and the $V_{1/2}$ values are shown in Table 1. Data are expressed as the mean ± SEM (n = 6–8).

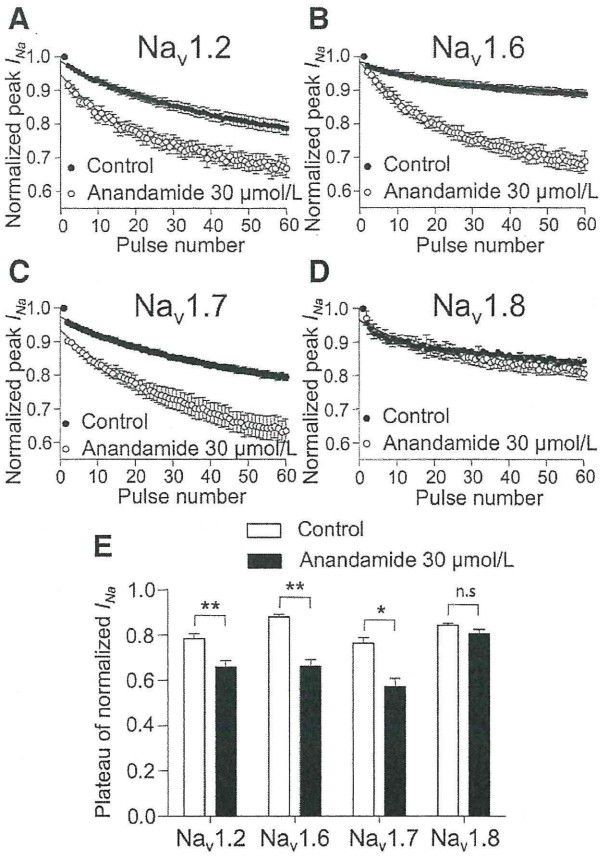

Figure 7. Use-dependent block of sodium channel on $Na_v1.2$, $Na_v1.6$, $Na_v1.7$, and $Na_v1.8$ α subunits with β_1 subunits of anandamide. Currents were elicited at 10 Hz by a 20-millisecond depolarizing pulse of –20 mV for $Na_v1.2$ and $Na_v1.6$, or –10 mV for $Na_v1.7$, or +10 mV for $Na_v1.8$ from a $V_{1/2}$ holding potential in both the absence and presence of 30 μmol/L anandamide; anandamide was applied for 5 minutes. Peak currents were measured and normalized to the first pulse and plotted against the pulse number (A, $Na_v1.2$; B, $Na_v1.6$; C, $Na_v1.7$; D, $Na_v1.8$). Closed circles represent control; open circles indicate the effect of anandamide. Data were fitted to the monoexponential equation, and values for fractional block of the plateau of normalized I_{Na} are shown in (E). Data are expressed as the mean ± SEM (n = 5–6). *P < 0.05 and **P < 0.01, compared with the control (paired t test).

carrageenan,[51,52] whereas $Na_v1.7$ protein decreased in the injured DRG after spared nerve injury in animals.[53] $Na_v1.8$ mRNA and protein increased in DRG neurons of rodents after injection of carrageenan into a hindpaw,[51,54,55] and yet peripheral nerve injury down-regulates $Na_v1.8$ mRNA and protein expression in the injured DRG.[29,53,56] Based on this evidence, suppression of sensory neuron sodium channel function by anandamide may be an important mechanism independent of the cannabinoid receptor. Because of the limitations of our experiments, further investigation is warranted to extrapolate our findings into clinical practice.

In conclusion, anandamide at pharmacologically relevant concentrations inhibited sodium currents of $Na_v1.2$, $Na_v1.6$, $Na_v1.7$, and $Na_v1.8$ α subunits expressed in the *Xenopus* oocytes with differences in the effects on sodium channel gating. These results provide a better understanding of the mechanisms underlying the analgesic effects of anandamide, but further studies are needed to clarify the relevance of sodium channel inhibition by anandamide to analgesia.

DISCLOSURES

Name: Dan Okura, MD.

Contribution: This author helped data collection, data analysis, and manuscript preparation.

Attestation: Dan Okura approved the final manuscript and attests to the integrity of the original data and the analysis reported in this manuscript.